Supplementary Information

Chengyue Sun[a], Jiming Zheng[*,b], Sujuan Zhang[b], Zhaopu Ju[c], Aihua Gao[c], Ping Guo[c], Zhenyi Jiang[*,a]

Contents

[a] *Shaanxi Key Laboratory for Theoretical Physics Frontiers, Institute of Modern Physics, Northwest University, Xi'an 710069, China.E-mail:jiangzy@nwu.edu.cn*

[b] *National Key Laboratory of Photoelectric Technology and Functional Materials (Culture Base) in Shaanxi Province,Northwest University, Xi'an 710069, China.E-mail:zjm@nwu.edu.cn*

[c] *Department of Physics, Northwest University, Xi'an 710069,China.*

1 The optimized lattice structure parameters of 1T'

Table S-1: The optimized lattice structure parameters of 1T'(in $\mathring{A}$).

Pristine	MoS_2	$MoSe_2$	$MoTe_2$	WS_2	WSe_2	WTe_2
a	5.72	5.98	6.34	5.72	5.94	6.33
b	3.18	3.28	3.47	3.19	3.30	3.49

Janus	$MoSTe$	$MoSeTe$	$WSTe$	$WSeTe$
a	6.09	6.19	6.06	6.15
b	3.34	3.37	3.34	3.41

2 Total energy and formation energy of TMDs

Table S-2: Total energy and formation energy of TMDs.

		$MoTe_2$	$MoSeTe$	$MoSTe$	$WSeTe$	$WSTe$
Total energy	E_{2H}/eV	-18.0295	-18.924	-19.597	-20.4378	-21.327
	$E_{1T'}$/eV	-17.9885	-18.755	-19.468	-20.3608	-21.142
Formation energy	E_{2H}/eV	-12.1162	-12.886	-13.454	-14.4598	-15.246
	$E_{1T'}$/eV	-12.0752	-12.717	-13.325	-14.3828	-15.061

3 TB parameters selection range

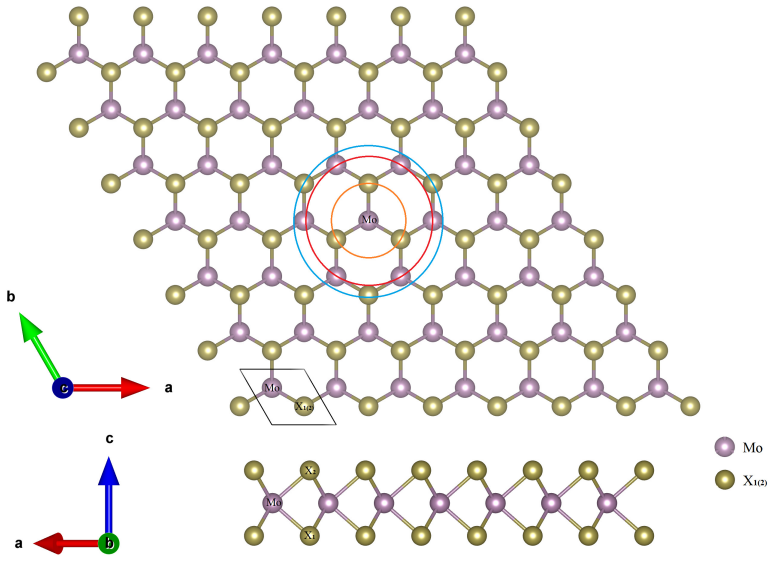

Figure S-1: The lattice structure of a single layer of MoX_2 (purple sphere represents Mo atom and yellow sphere represents X atom) contains three atoms in the unitcell, respectively Mo and $X_{1(2)}$. (a) Take the Mo atom as an example, neighboring atoms are at most the third nearest neighbor, and the centers are indicated by yellow (first nearest neighbors), red (second nearest neighbors), and light blue (third nearest neighbors).(b) Side view of monolayer MoX_2(X=Te/Se/S).

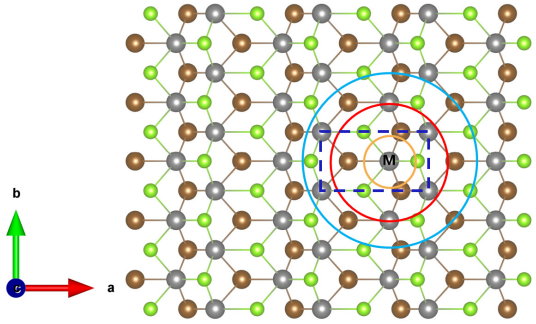

(a)

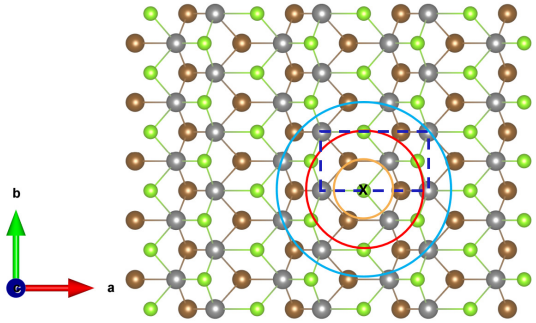

(b)

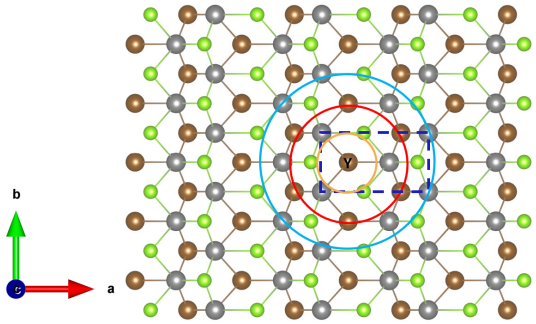

(c)

Figure S-2: The lattice structure of monolayer MXY (gray sphere represents M, green sphere represents X atom, brown sphere represents Y atom) contains six atoms in the protocell, namely $M_{1(2)}$, $X_{1(2)}$ and $Y_{1(2)}$.For (a) M atoms, (b) X atoms, and (c) Y atoms whose neighbors are at most third nearest neighbors, the centers are indicated by yellow (first nearest neighbor), red (second nearest neighbor), and light blue (third nearest neighbor), respectively.(d) Side view of monolayer MXY.

4 Fitting parameters of MXY(M=W, Mo;X/Y=Se, Te)

Table S-3: MXY(M=W, Mo;X/Y=Se, Te) parameters of the first nearest neighbor dynamic matrix model.

			$MoTe_2$	$WSeTe$	$WSTe$	$MoSTe$	$MoSeTe$
Out-of-plane	$X_1 - Y_1$	$V_{pp\sigma 1}$	7.5841	15.6465	7.8743	14.7706	8.6776
		$V_{pp\pi 1}$	-0.1654	0.5387	2.3836	2.6957	3.2565
	$X_1 - Y_2/X_2 - Y_1$	$V_{pp\sigma 2}$	20.7083	3.9916	3.0706	3.5747	20.8520
		$V_{pp\pi 2}$	3.8745	1.4242	0.7444	4.44331	-3.9335
	$X_2 - Y_2$	$V_{pp\sigma 3}$	7.0054	8.3224	17.2694	5.9900	13.1089
		$V_{pp\pi 3}$	0.2908	0.5833	-1.8288	-1.7639	3.4387
	$X_{1(2)} - M_{1(2)}$	$V_{pp\sigma 4}$	0.1794	1.4251	2.3680	-0.2794	3.9624
		$V_{pp\pi 4}$	0.1194	3.8004	8.2073	8.0139	2.6050
	$Y_{1(2)} - M_{1(2)}$	$V_{pp\sigma 5}$	-5.1627	4.6504	-8.6380	-10.7673	0.4169
		$V_{pp\pi 5}$	5.5244	0.0784	6.6057	7.5964	1.4196
Inplane	$M_1 - M_2$	$V_{pp\sigma 6}$	1.5545	4.0503	26.8723	35.6964	0.0289
		$V_{pp\pi 6}$	0.9398	-1.7139	4.0564	0.2135	-1.2943
	$Y_1 - Y_2$	$V_{pp\sigma 7}$	4.6523	2.1805	1.4887	7.5153	4.9987
		$V_{pp\pi 7}$	0.7135	-0.6878	0.1226	0.7211	-1.3385
	$X_1 - X_2$	$V_{pp\sigma 8}$	2.2235	1.9026	-3.0986	-2.0698	9.7119
		$V_{pp\pi 8}$	-0.9378	0.3071	-2.3747	-2.9849	0.6259
Self-force constant	$Y_1 - Y_1/Y_2 - Y_2$	$V_{pp\sigma 9}$	1.2420	0.3463	1.6763	3.9529	-0.5750
		$V_{pp\pi 9}$	1.4451	-0.9983	0.3224	2.2945	4.7390
	$X_1 - X_1/X_2 - X_2$	$V_{pp\sigma 10}$	-0.1709	-2.6013	-0.5585	0.1863	4.5585
		$V_{pp\pi 10}$	-1.8618	3.5542	-1.3013	-1.5125	-5.3850
	$M_1 - M_1/M_2 - M_2$	$V_{pp\sigma 11}$	1.1704	2.4871	-5.5559	-4.3569	3.3991
		$V_{pp\pi 11}$	1.8960	0.4497	10.8445	6.3181	0.5462

Table S-4: MXY(M=W, Mo;X/Y=Se, Te) parameters of the second nearest neighbor dynamic matrix model.

			$MoTe_2$	$WSeTe$	$WSTe$	$MoSTe$	$MoSeTe$
Out-of-plane	$X_1 - Y_1$	$V_{pp\sigma 1}$	0.6842	1.4097	0.7053	1.3085	0.7902
		$V_{pp\pi 1}$	-0.0149	0.0485	0.2135	0.2388	0.2965
	$X_1 - Y_2 / X_2 - Y_1$	$V_{pp\sigma 2}$	2.8105	0.5364	0.4086	0.4792	2.8219
		$V_{pp\pi 2}$	0.5267	0.1914	0.0990	0.5956	-0.5323
	$X_2 - Y_2$	$V_{pp\sigma 3}$	0.8081	0.9518	1.9487	0.6761	1.4990
		$V_{pp\pi 3}$	0.0335	0.0667	-0.2064	-0.1991	0.3932
	$Y_2 - M_1$	$V_{pp\sigma 4}$	-0.5086	0.7852	-0.8846	-1.1139	0.0423
		$V_{pp\pi 4}$	0.5443	0.0132	0.6765	0.7859	0.1440
	$Y_1 - M_2$	$V_{pp\sigma 5}$	-0.6058	0.5479	-1.0073	-1.2373	0.0481
		$V_{pp\pi 5}$	0.6482	0.0092	0.7703	0.8729	0.1639
	$Y_2 - M_2$	$V_{pp\sigma 6}$	-0.3234	0.3028	-0.5777	-0.7233	0.0273
		$V_{pp\pi 6}$	0.3461	0.0051	0.4418	0.5103	0.0931
	$Y_1 - M_1$	$V_{pp\sigma 7}$	-0.3916	0.2793	-0.6898	-0.8503	0.0326
		$V_{pp\pi 7}$	0.4190	0.0047	0.5275	0.5999	0.1109
	$X_1 - M_2$	$V_{pp\sigma 8}$	0.0136	0.0997	0.1532	-0.0185	0.2763
		$V_{pp\pi 8}$	0.0091	0.2659	0.5309	0.5301	0.1816
	$X_1 - M_1$	$V_{pp\sigma 9}$	0.0211	0.0558	0.2768	-0.0324	0.4583
		$V_{pp\pi 9}$	0.0140	0.1489	0.9594	0.9292	0.3012
	$X_2 - M_2$	$V_{pp\sigma 10}$	0.0177	0.1355	0.2185	-0.0256	0.3788
		$V_{pp\pi 1-}$	0.0118	0.3614	0.7572	0.7335	0.2489
	$X_2 - M_1$	$V_{pp\sigma 11}$	0.0112	0.2137	0.1306	-0.0153	0.2333
		$V_{pp\pi 11}$	0.0075	0.5699	0.4526	0.4380	0.1533
Inplane	$X_1 - X_2$	$V_{pp\sigma 12}$	0.3986	0.3489	-0.5620	-0.3754	1.74444
		$V_{pp\pi 12}$	-0.1681	0.0555	-0.4307	-0.5414	0.1124
	$Y_1 - Y_2$	$V_{pp\sigma 13}$	0.4301	0.1997	0.1366	0.6921	0.4621
		$V_{pp\pi 13}$	0.0660	-0.0630	0.0112	0.0664	-0.1237
	$M_1 - M_2$	$V_{pp\sigma 14}$	0.1690	1.4555	3.1028	4.0833	0.0033
		$V_{pp\pi 14}$	0.1022	-0.6159	0.4684	-0.0244	-0.1463

Table S-5: MXY(M=W, Mo;X/Y=Se, Te) parameters of the third nearest neighbor dynamic matrix model.

			$MoTe_2$	$WSeTe$	$WSTe$	$MoSTe$	$MoSeTe$
Out-of-plane	$Y_1 - M_2$	$V_{pp\sigma 1}$	-0.5086	0.7852	-0.8846	-1.1139	0.0423
		$V_{pp\pi 1}$	0.5443	0.0132	0.6765	0.7859	0.1440
	$M_1 - Y_2$	$V_{pp\sigma 2}$	-0.3865	1.6586	-0.6930	-0.8705	0.0325
		$V_{pp\pi 2}$	0.4136	0.0280	0.5300	0.6141	0.1105
	$Y_1 - M_1$	$V_{pp\sigma 3}$	-0.3455	0.5955	-0.6135	-0.7567	0.0292
		$V_{pp\pi 3}$	0.3697	0.0100	0.4692	0.5339	0.0994
	$X_1 - M_1$	$V_{pp\sigma 4}$	0.0184	0.1888	0.2340	-0.0277	0.4011
		$V_{pp\pi 4}$	0.0123	0.5035	0.8112	0.7957	0.2636
	$X_2 - M_2$	$V_{pp\sigma 5}$	0.0134	0.1059	0.1715	-0.0196	0.2896
		$V_{pp\pi 5}$	0.0089	0.2825	0.5945	0.5630	0.1903
	$X_1 - M_2$	$V_{pp\sigma 6}$	0.0120	0.0887	0.1393	-0.0168	0.2501
		$V_{pp\pi 6}$	0.0080	0.2367	0.4827	0.4820	0.1649
Inplane	$M_1 - M_2$	$V_{pp\sigma 7}$	0.1078	0.6431	1.9126	2.5447	0.0021
		$V_{pp\pi 7}$	0.0652	-0.2721	0.2887	-0.0152	-0.0923

5 Phonon spectrum and DOS of other TMDs under $1T'$ phase

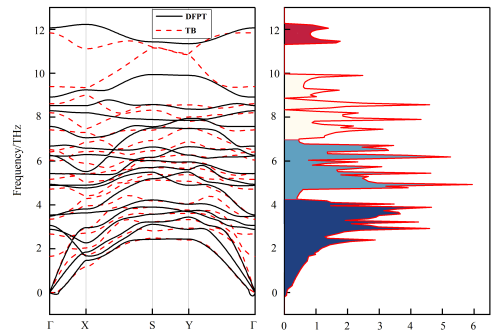

(a)

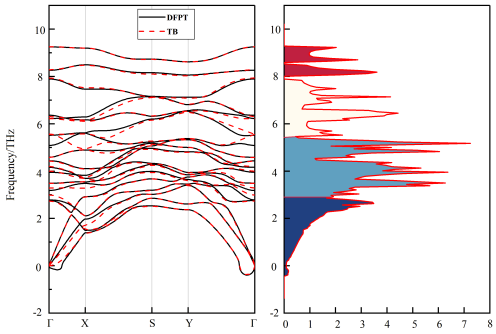

(b)

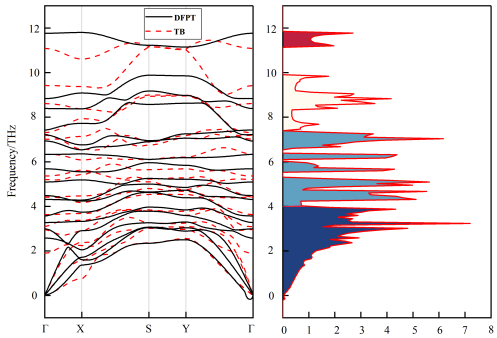

(c)

Figure S-3: Phonon spectrum and phonon DOS of TMDs under 1T' phase. (a) $1T' - MoSTe$ (b) $1T' - MoSeTe$ (c) $1T' - WSTe$.The black solid line depicts the phonon spectrum obtained by DFPT calculation, and the red dotted curve depicts the phonon spectrum obtained by TB model.The DOS of the structures are shown on the right.

6 Estimate of the error bars in the free energy calculations and the transition temperature

Based on our knowledge about error theory, there are mainly two sources of error. One is the systematic error and the other is random error. In this work, the systematic error comes from the other interaction energies not considered in the DFT calculations, such as the energy change of electrons with their temperature rising, the electron-phonon interaction, and so on.

Following the reviewer's advice, we attempt to estimate the magnitude of one part of these errors. At temperature T, The intrinsic carrier concentration for a semiconductor is

$np = 4(\frac{K_B T}{2\pi\hbar^2})^3 (m_e m_h)^{3/2} exp(-Eg/k_B T)$ (Introduction to solid state physics, by Charles Kittel, here, n and p are dengsity of electron and hole, m_e, and m_h are effective mass of electron and hole, respectively.) After simple calculations, we conclude that the carrier density of the $2H - MoTe_2 (Eg = 1.04eV)$ is about $10^9 cm^{-3}$ (at 300K) and $10^{16} cm^{-3}$ (at 900K). While, there are 2.77×10^{23} cells (lattice constant is in Table.S1 in SI) in the one cubic centimeter. Thus, every 10^{14} cells at $T = 300K$, and 10^7 cells at $T = 900k$ will afford one excited electron. Considering that all the energy items used in the free energy calculation are based on one unitcell, this kind of energy change, calculated as each excited electron contribute one band gap energy (Eg) to the total energy U, is very small ($10^{-14} - 10^{-7} eV$).

Similar estimation can be done for $1T'$ phase which show metallic features. Here, the total energy change caused by temperature rising is

$\Delta U = \int_{E_f}^{\infty} d\epsilon(\epsilon - E_f) f(\epsilon) g(\epsilon) + \int_0^{E_f} d\epsilon(\epsilon - E_f)[1 - f(\epsilon)] g(\epsilon)$.

The first item in the right side of the above equation represent the energy to excite the electron at E_F to levels above the E_F, and the last item represent the energy to excite the electron below E_F to the E_F. The contribution form the temperature excitation to the total energy is about $0.006eV$, and $0.002eV$ at $T = 900K$ for $1T' - MoTe_2$ and $1T' - WSeTe$, respectively. Through calculation, the change of total energy in this part corresponds to the change of phase transition temperature of 144K and 17K for $1T' - MoTe_2$ and $1T' - WSeTe$, respectively.

If carriers induced by dopant are important, the total energy change of electron system will depend on the density of carriers. Beacause of the lack of the dopant information, the influence of the doped carrier on the total energy of the system with the change of temperature is not included in this paper, and further study is needed.

Based on the above error analysis, we find that the systematic error induced phase transition temperature fluctuation is in the order of 100K and 10K for $MoTe_2$ and $WSeTe$, respectively.

7 The bader charge analysis of $1T' - WSeTe$ and $1T' - MoTe_2$

From the Fig S-1, one can observe that chalcogenide atoms in Janus TMDs show a relatively larger variation in bader charge. The charge transfer between metal and nonmetallic atoms means that the bond formed between them has the ionic bonds feature, and also indicates that the interaction between metal and nonmetallic atoms is the strongest, which will lead to the highest frequency of relative vibration between metal and nonmetallic atoms. And it is also consistent with our calculated phonon spectrum.

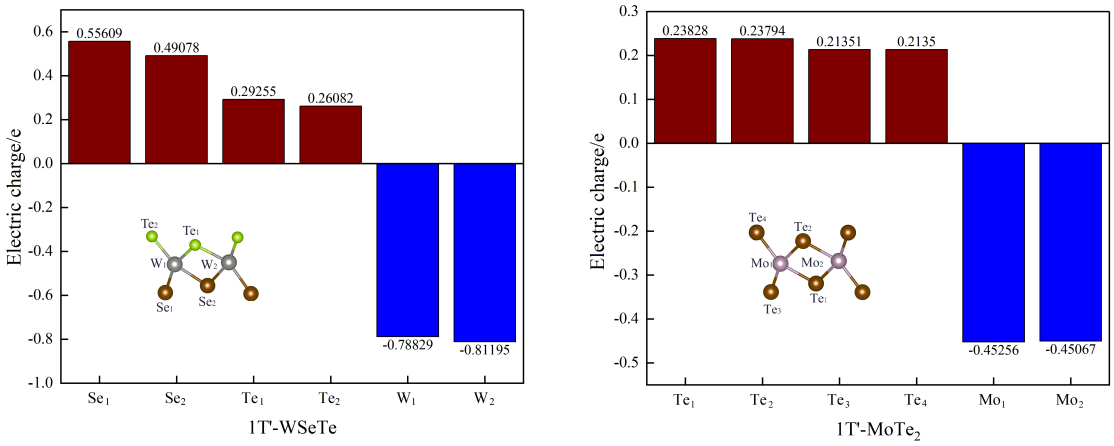

Figure S-4: The bader charge of $1T' - WSeTe$ and $1T' - MoTe_2$.

8 The energy gradients of the F_T part of TMDs

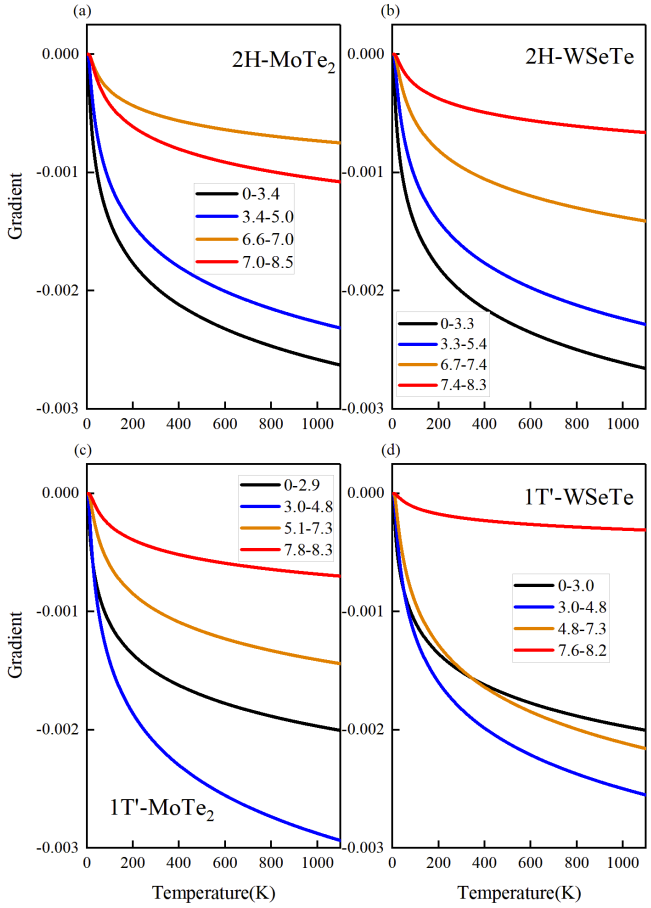

Figure S-5: (a),(b),(c) and (d) are the energy gradients of the F_T part of $2H - MoTe_2$, $2H - WSeTe$, $1T' - MoTe_2$, $1T' - WSeTe$, respectively. Black, blue, orange and red represent the gradient change of F_T in four energy intervals from low to high respectively.